A motif in the 5'untranslated region of messenger RNAs regulates protein synthesis in a S6 kinase-dependent manner.

Hyun-Chul Shin, Yury A Bochkov, Kangsan Kim, James E Gern, Nizar N Jarjour, Stephane Esnault

Advances in Biological Regulation 89 (2023) 100975

Contents lists available at ScienceDirect

Advances in Biological Regulation

journal homepage: www.elsevier.com/locate/jbior

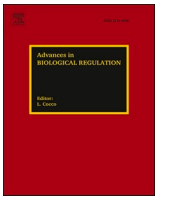

A motif in the 5′untranslated region of messenger RNAs regulates protein synthesis in a S6 kinase-dependent manner

Hyun-Chul Shin [a,1], Yury A. Bochkov [b,1], Kangsan Kim [a], James E. Gern [b,c], Nizar N. Jarjour [c], Stephane Esnault [c,*]

[a] Department of Chemistry Education, Korea National University of Education, Cheongju-si, Chungcheonbuk-do, Republic of Korea
[b] Department of Pediatrics, School of Medicine and Public Health, University of Wisconsin, Madison, WI, USA
[c] Department of Medicine, School of Medicine and Public Health, University of Wisconsin, Madison, WI, USA

ARTICLE INFO

Handling Editor: Dr. L. Cocco

Keywords:
mRNA translation
Protein synthesis
5′ untranslated region
S6 kinase
Eosinophils

ABSTRACT

The 5′ untranslated regions (UTRs) in messenger RNAs (mRNAs) play an important role in the regulation of protein synthesis. We had previously identified a group of mRNAs that includes human semaphorin 7A (SEMA7A) whose translation is upregulated by the Erk/p90S6K pathway in human eosinophils, with a potential negative impact in asthma and airway inflammation. In the current study, we aimed to find a common 5′UTR regulatory cis-element, and determine its impact on protein synthesis. We identified a common and conserved 5′UTR motif GGCTG—[(C/G)T(C/G)]$_n$—GCC that was present in this group of mRNAs. Mutations of the first two GG bases in this motif in SEMA7A 5′UTR led to a complete loss of S6K activity dependence for maximal translation. In conclusion, the newly identified 5′UTR motif present in SEMA7A has a critical role in regulating S6K-dependent protein synthesis.

1. Introduction

Fine-tuning of protein production in response to environmental and signaling changes is essential for optimal maintenance of cell and tissue homeostasis. Protein synthesis starts by the binding of multiple eukaryotic translation initiation factors to the mRNA 5′-cap that likely unwind some secondary structures such as GC-rich structures in the 5′- untranslated region (5′ UTR) (Pelletier and Sonenberg, 1985), thus facilitating mRNA translation. Multiple studies have shown that a secondary structure and protein interactions in the 5′ UTR generally control the efficiency of ribosome scanning to the start codon (Ding et al., 2014; Taliaferro et al., 2016; Tuller and Zur, 2015; Wan et al., 2014). Given the limitations of predicting global 5′ UTR mRNA structures, the search for individual functional mRNA structures may be more appropriate to identify the structures involved in the control of mRNA translation. Recent studies suggest that the function of eIF4A in binding and unwinding RNA can have specific effects on target mRNAs, at least in part through structured RNA elements in 5′ UTRs (Rubio et al., 2014). Depending on stimulus and cell type, modified RNA-binding proteins (RBPs) associate with or dissociate from mRNAs, affecting the transcripts' stability as well as their translation into proteins. RBPs bind to RNA via a variety of domains, called RNA-recognition motifs (RRMs) (Glisovic et al., 2008). Selective mRNA/RBP interaction requires the recognition of unique cis-regulatory elements and/or structures within the mRNA. In this way, subsets of mRNAs can be

* Corresponding author.
E-mail address: sesnault@wisc.edu (S. Esnault).
[1] Co-first authors.

https://doi.org/10.1016/j.jbior.2023.100975
Received 6 March 2023; Accepted 5 June 2023
Available online 7 June 2023

selectively identified and regulated for differential translation and mRNA decay. One well-studied example is the mTOR-regulated pyrimidine-rich domain termed terminal oligopyrimidine (TOP) (Jefferies et al., 1994; Thoreen et al., 2012). Due to the large number of already known RBPs, it is likely that many RNA-recognition elements in the 5′UTRs remain to be discovered.

RPS6 is a component of the 40S ribosomal subunit, and its phosphorylation at Ser(235/236) by p90S6 kinase promotes its recruitment to the 7-methylguanosine cap complex, suggesting that phosphorylated RPS6 regulates assembly of the translation pre-initiation complex (Roux et al., 2007). We have previously shown that IL-3 prolonged Erk/p90S6K signaling leading to increased SEMA7A protein translation without significant increase of mRNA amount in activated human blood eosinophils, between 4 h and 20 h after activation (Esnault et al., 2015), indicating that SEMA7A protein was increased by regulation(s) at the translational level. SEMA7A is highly expressed on activated T lymphocytes, and its localization in the immunological synapse amplifies pro-inflammatory cytokine expression by antigen-presenting cells (Suzuki et al., 2007). In addition, SEMA7A participates in the induction of pulmonary fibrosis (Kang et al., 2007; Reilkoff et al., 2013); and in eosinophils, SEMA7A leads to adhesion to plexin C1 and to increased alpha-smooth muscle actin production in human bronchial fibroblasts (Esnault et al., 2014). Therefore, identifying mechanisms involved in the post-transcriptional regulation of SEMA7A is important because SEMA7A may increase lung tissue remodeling and airway inflammation in asthma.

We also reported that, similarly to SEMA7A, Fc gamma receptor IIb (FCGR2B) was regulated by IL-3 at the translational level by the same ribosomal protein S6 kinase (Esnault et al., 2017a, 2018). Furthermore, SEMA7A and transforming growth factor alpha (TGFA) mRNAs, but not the TOP mRNAs were enriched in polyribosomes in IL3-activated eosinophils compared to non-activated eosinophils (Esnault et al., 2015), suggesting a unique and selective signaling from the IL-3 receptor to the translational machinery for specific mRNAs, such as SEMA7A, FCGR2B and TGFA mRNAs.

Therefore, in the current study, we tested for a cis-regulatory motif in the 5′UTR of SEMA7A that could be responsible for the regulation of mRNA translation in a S6K-dependent manner.

2. Methods

2.1. SEMA7A cDNA constructs

Expression-ready cDNA clone for SEMA7A in pTCN vector (TransOMIC Technologies, Huntsville, AL), designated pTCN-SEMA7A, used in this study has been previously described (Esnault et al., 2017b). Since the 5′UTR SEMA7A sequence was incomplete and 3′ UTR was lacking a poly(A) sequence in pTCN-SEMA7A plasmid, we constructed a wild-type (GG) and mutated (AA) 5′UTR plasmids with the poly(A) sequences for SEMA7A protein expression. First, pSEMA7A-poly(A) was made by linking the purified PCR product obtained using the primers shown in Table S1 and pTCN-SEMA7A vector via BstEII and HindIII restriction sites. Next, the GG (wild-type) and AA (mutated) versions of pSEMA7A were engineered by PCR using the appropriate forward primers with the wild-type or mutated bases and reverse primer Sema7A-PasI (Table S1) following ligation via BamHI and PasI restriction enzyme sites. All plasmid DNAs were verified in the regions of interest by sequencing, and then purified by Plasmid Maxi kits (Qiagen).

2.2. SEMA7A-eGFP cDNA constructs

We sought to construct eGFP reporter plasmids that contain wild-type SEMA7A 5′UTR (5′UTR-SEMA7A) sequence and different mutations upstream of the start codon of eGFP gene. The pcDNA3-eGFP plasmid was from Addgene (Watertown, MA, USA). First, we inserted a synthesized oligomer cassette (5′-agcttgctagccccaccggtccacccat-3′ and 5′-gtggaccggtggggctagca-3′) that includes HindIII-NheI-AgeI-BstXI between the initiator element (Inr)+1 site and the start codon of pCDNA3-eGFP using HindIII and BstXI digestion. To construct wild-type and mutated 5′UTR-SEMA7A sequences, we synthesized 44-mer of forward and reverse DNA sequences for wild-type, mutant 1 (M1), mutant 2 (M2), mutant 3 (M3) and double mutant M1M2 and M1M3, with protruding ends (NheI for forward and AgeI for reverse) as shown in Table S2. Oligomers were annealed, then introduced into NheI and AgeI-digested pcDNA3-eGFP plasmid to construct SEMA7A-eGFP or a series of SEMA7A-mutant-eGFP plasmids.

2.3. Cell culture and transfection

For Fig. 4, HeLa–H1 (ATCC# CRL-1958) cells were grown in Eagle's Minimum Essential Medium (EMEM, Lonza) supplemented by non-essential amino acids (Gibco) and 10% fetal bovine serum (Gemini). The transfection-grade plasmid DNAs were prepared by Plasmid Maxi kit (Qiagen) and transfected into monolayers of HeLa cells in 12-well plates using Lipofectamine 2000 (Life Technologies) according to the manufacturer's instructions. For Fig. 5, HeLa cells were purchased from the Korean Cell Line Bank (Seoul, South Korea) and maintained in EMEM (HyClone™, Cytiva Life science, MA, USA) supplemented with 2 mM L-Glutamine, 500 unit/mL Penicillin, 500 μg/mL Streptomycin, 10% FBS. All the reagents were purchased from HyClone™. (Cytiva Life science, MA, USA). HeLa cells were seeded in 24-well culture plates (SPL life Science, Gyeonggi, Korea) 24 h prior to transfection with 2 μg of plasmids complexed with 8 μg of polyethylenimine. The culture media were changed with fresh DMEM (2 mM L-Glutamine, 500 unit/mL Penicillin, 500 μg/mL Streptomycin, 10% FBS). Transfection efficiencies were between 20 and 25% as evaluated from pcDNA-eGFP plasmid at 24 h post-transfection. To inhibit S6K activity, cells were treated with 15 μM PF-4708671(Calbiochem, CA, USA) 6 h prior transfection. The same concentration of S6K inhibitor was added to cells when culture medium was changed.

2.4. Western-blot and qPCR for SEMA7A

Western blots were performed as previously described (Esnault et al., 2017b). Briefly, HeLa cells were lysed directly in Laemmli buffer (10% SDS) before boiling for 5 min and loading onto a 10% SDS-PAGE gel. Mouse monoclonal antibodies against β-actin and the rabbit polyclonal anti-mouse SEMA7A antibody were from Sigma and Abgent (San Diego, CA), respectively. Rabbit monoclonal antibodies anti-RPS6-S235/236 was from Cell Signaling. Secondary HRP-conjugated anti-rabbit IgG Ab and anti-mouse IgG Ab were from Pierce/Thermo Fisher Scientific (Rockford, IL) (anti-rabbit), from Amersham-GE Healthcare Life Sciences (Chicago, IL) or from Calbiochem (anti-mouse). Immunoreactive bands were visualized with Super Signal West Femto chemiluminescent substrate (Pierce/-Thermo Fisher Scientific). Bands were quantified using the FluorChem®Q Imaging System (Alpha Innotech/ProteinSimple, Santa Clara, CA, USA), and data are expressed as a ratio of target to β-actin.

RNA extraction and quantitative PCR were performed as previously described (Esnault et al., 2014). Briefly, total RNA was extracted from HeLa cells using the RNeasy Mini Kit (Qiagen, Valencia, CA, USA). The reverse transcription reaction was performed using the Superscript III system (Invitrogen/Life Technologies, Grand Island, NY, USA). mRNA expression was determined by real-time quantitative PCR (RT-qPCR) using SYBR Green Master Mix (SABiosciences, Frederick, MD, USA) and human SEMA7A forward (CTCCGCCCAGGGCCACCTAA) and reverse (ACATGGCCTTTCCAGACGGCG) specific primers. The ß-glucuronidase (GUSB) gene, amplified with the forward: CAGGACCTGCGCACAAGAG, reverse: TCGCACAGCTGGGGTAAG primers, was used to normalize the SEMA7A gene expression. Applied Biosystems (ABI/Invitrogen, Carlsbad, CA, USA) 7500 Sequence detector was used. Standard curves were performed, and efficiencies were determined for each set of primers. Efficiencies ranged between 93 and 96%. Data are expressed as fold change using the comparative cycle threshold (ΔΔCT) method.

2.5. Quantification of eGFP protein production

The fluorescent images were acquired from live HeLa cell culture (magnification of objective x4, GFP LED cube (482/524 nm) at the indicated timepoints post-transfection using fluorescence microscope (EVOS M5000 imaging system, Thermo Fischer, MA, USA). For the accuracy of analysis, setting of the fluorescent microscope at the acquisition remained fixed for all samples and experiments. Single experiments comprised 5 individual wells per plasmid, and 3 independents experiments were performed. All the images were captured at the center of culture plates and saved as 16-bit TIFF format. Each image was processed to measure total area of fluorescence and the mean grey scale to calculate average intensity of fluorescence using ImageJ v1.53k (https://imagej.nih.gov/ij/).

2.6. Statistical analysis

Statistical analyses were performed using the SigmaPlot 13.0 software package (Systat Software, Inc., Palo Alto, CA, USA). Differences between 2 groups were analyzed using Student's *t*-test as indicated in the figures. Student's *t*-test was followed by the Mann-Whitney Rank Sum test if values did not have a normal distribution. Groups are different for P values <0.05.

3. Results

3.1. SEMA7A, FCGR2B (CD32), TGFA and some other mRNAs display a common motif in their 5′UTRs

We found a motif of 23–34 nucleotides that starts with GGCTG, ends with GCC and exhibits (C/G)T(C/G) repeats in the 5 'UTR upstream of the start codon of SEMA7A, FCGR2B and TGFA mRNAs (Fig. 1). To find more transcripts with this motif, we combined transcriptomic [RNA sequencing values deposited to the NCBI Gene Expression Omnibus (GEO) database and assigned Accession Number (**GSE159782**)] and proteomic analyses [proteins listed in supplemental spreadsheet 1 in ref (Esnault et al., 2018).] of IL3-activated versus non-activated human blood eosinophils. First, among the statistically significant (adjusted q value <0.05) upregulated 1150 proteins in IL3-activated eosinophils, we extracted 200 proteins whose amounts were the most increased by IL3 treatment for 20 h. Second, using the transcriptomic database, we extracted the genes that showed expression level enhanced by $>$ 2-fold at either 4 h, 20 h or both in IL3-activated eosinophils versus non-activated eosinophils, as for previously reported SEMA7A and FCGR2B mRNAs (Esnault et al., 2015, 2017a). Among the 828 genes responding to this profile of expression, 74 genes were also

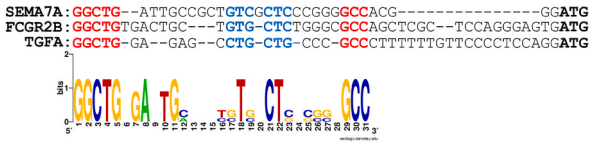

Fig. 1. Identification of an apparent common motif in the 5′UTR of SEMA7A, FCGR2B and TGFA. The 5′UTR of each of the genes, which are known to be upregulated at the translation level in IL3-activated eosinophils and associated with continuous activation of the Erk/p90S6K pathway, were manually aligned. NCBI Reference Sequences: NM_003612.5 for SEMA7A; NM_004001.5 for FCGR2B and NM_003236.4 for TGFA. Nucleotides in red represent the beginning and the end of the conserved motif, while in blue are highly conserved regions in the center of the motif. Frequency of nucleotides in the motif was analyzed using WebLogo (https://weblogo.berkeley.edu/) from Gavin E. Crooks, Gary Hon, John-Marc Chandonia and Steven E. Brenner, Computational Genomics Research Group, Department of Plant and Microbial Biology, University of California, Berkeley.

included in the top 200 proteins the most upregulated by IL3 treatment. Because the mRNA expression levels of SEMA7A and FCGR2B were not changed between 4 h and 20 h in IL3-activated eosinophils (Esnault et al., 2015, 2017a), we thus looked for genes whose expression level ratio between 4 h and 20 h was close to 1. Among the 74 genes, we found 20 genes with expression level ratio (20 h/4 h) comprised between 1.4 and 0.8. Of these 20 genes, 9 displayed a motif similar to GGCTG—[(C/G)T(C/G)]$_n$—GCC in their 5'UTR. As expected, among these 9 genes, SEMA7A and FCGR2B were present (Fig. 2A). TGFA was not present because TGFA is a secreted protein that was not detected by the cellular proteomic experiment. Hence, using this method, we identified CD58, IDI1, KIF21B, NFE2, SEC16A, SLC29A1 and SNX10 as having a similar GGCTG—[(C/G)T(C/G)]$_n$—GCC motif in their 5′UTR, with sizes ranging between 25 and 58 nucleotides (https://www.ncbi.nlm.nih.gov/gene/). Among the 11 remaining genes, IL1RAP displayed the GGCTG—CTG—GCC motif, but lack the repeats of [(C/G)T(C/G)], and FCGR2A did not display this motif, in agreement with one of our previous reports where unlike FCGR2B, FCGR2A protein amount was not dependent on IL3-induced prolonged Erk/p90S6K signaling in eosinophils (Esnault et al., 2017a). Remarkably, among the 74 genes, none of the 15 genes with mRNA expression level ratio (20 h/4 h) >3, possessed this motif (Fig. 2B). In summary, we identified seven new genes possessing GGCTG—[(C/G)T(C/G)]$_n$—GCC in their 5′ UTR and our data suggest an association between that motif with enhanced mRNA translation.

3.2. The start of the newly identified motif controls mRNA translation in an S6K-dependent manner

Notably, the SEMA7A sequence is well-conserved among mammals, particularly in primates and horses, and the beginning of the motif (GGCTG) identified in human SEMA7A is also found in other mammal and avian species (Fig. 3). Therefore, to demonstrate the importance of the first nucleotides of this motif in the S6K-dependent regulation of SEMA7A protein production, our first approach was to mutate **GG**CTG to **AA**CTG. We transfected HeLa cells, that did not express SEMA7A but displayed continuous p70S6k/RPS6-phosphorylation signaling (Fig. 4A), with a plasmid coding for the wild-type SEMA7A-GG or mutated SEMA7A-AA. Cells were pre-treated or not with an inhibitor of p70S6K (PF-4708671), which caused RPS6 de-phosphorylation. Translation of the wild-type SEMA7A-GG mRNA was reduced by S6K inhibition whereas translation of the mutated SEMA7A-AA was not affected by S6K activity (Fig. 4B). The expression level of the wild-type SEMA7A mRNA was not changed by S6K inhibition (Fig. 4C). These data indicate that the wild-type SEMA7A-GG is up-regulated by S6K, and in the absence of S6K/RPS6 signaling, the sequence starting with GGCTG acts as an inhibitor of SEMA7A protein synthesis. To further demonstrate a regulatory role of the GGCTG—[(C/G)T(C/G)]n—GCC motif in protein synthesis via S6K in trans, our second approach was to insert the 5′UTR of SEMA7A mRNA (41 nucleotides) in front of the coding region of enhanced green fluorescent protein (eGFP). Mutations were made at the start of the 5′UTR motif (mutation 1 [M1] or GG- > AA as in Fig. 5), in the following GC (M2) and in CTG (M3) (Fig. 5A). In addition, two double mutations were created with mutation 1 (M1M2 and M1M3; Fig. 5A). The 5′UTR-SEMA7A-eGFP wild-type and mutated plasmids were transfected in HeLa cells with or without a pre-treatment with the inhibitor of p70S6K (PF-4708671). The results have shown that only the double mutation M1 and M2 led to S6K-indepent translation (Fig. 5B). Therefore, in contrast to its cognate SEMA7A (Fig. 4), mutation 1 was not sufficient to enable S6K-independent protein production in trans for eGFP. To explain this discrepancy, we used an RNA-folding tool to predict secondary structures of the wild-type 5′UTR-SEMA7A and 5′UTR-SEMA7A-eGFP. Of note, compared to 5′UTR-SEMA7A, 5′UTR-SEMA7A-eGFP wild-type included an extra nucleotide sequence between the 5′UTR of SEMA7A and its start codon, composed of a cloning site for AgeI and a preexisting Kozak sequence (CCACCCAT) (Fig. 5A and C). Fig. 5C shows that mutation 1 can disrupt the first small stem-loop in the 5′UTR of SEMA7A while 5′UTR-SEMA7A-eGFP may require both mutations 1 & 2 to disrupt its long double-helix stem to loss the dependence for S6K activity. Thus, it is tempting to propose that these predicted hairpin loops at the beginning of the GGCTG—[(C/G)T(C/G)]n—GCC motif may cause the reduction of protein translation rate in the absence of S6K activity.

3.3. The newly identified element displays similarities with the small non-coding RNA, RNY3

We found that the 102-nucleotide sequence of a small non-coding RNA, RNY3, shows similarity with the GGCTG—[(C/G)T(C/G)]n—GCC motif. RNY3 full-length sequence starts with GGCTG and finishes with GCCTTTT, which likely confers RNY3 with the ability to

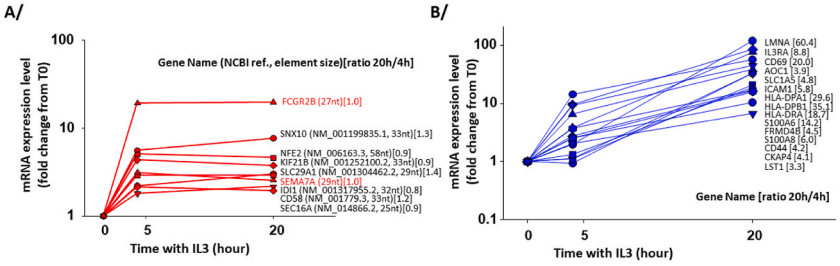

Fig. 2. Identification of other genes displaying the newly identified motif in their 5′UTR. We combined transcriptomic and proteomic analyses of IL3-activated versus non-activated human blood eosinophils to identify other IL3-upregulated genes at the protein and mRNA levels. **A/** Among 20 genes with a mRNA expression profile between 4 h and 20 h closely similar to previously reported SEMA7A and FCGR2B (i.e., ratio of 1), 11 displayed the GGCTG—[(C/G)T(C/G)]$_n$—GCC element in their 5′ UTR (https://www.ncbi.nlm.nihgov/gene/). **B/**Among 15 genes that unlike SEMA7A and FCGR2B showed significant increased mRNA expression (>3) between 4 h and 20 h, none displayed a GGCTG—[(C/G)T(C/G)]$_n$—GCC motif.

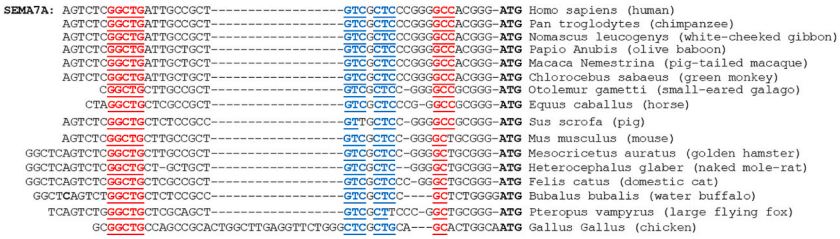

Fig. 3. Conservation of the 5′UTR motif in SEMA7A among different species. 5′UTR sequences from https://www.ncbi.nlm.nihgov/gene/. The underlined red and blue nucleotides represent the beginning, end and the conserved central region of the motif as shown in Fig. 2.

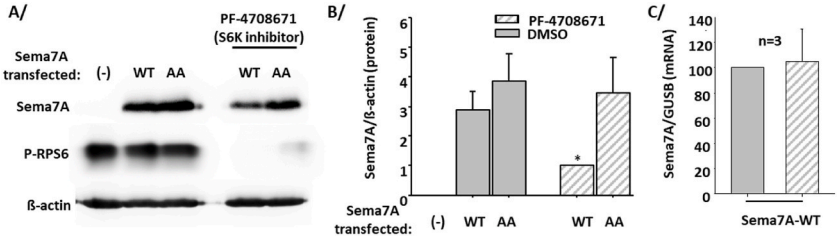

Fig. 4. Mutation (GG- > AA) at the beginning of regulatory sequence motif in SEMA7A 5′UTR leads to a loss of S6K-dependent translation of SEMA7A mRNA. HeLa cells were transfected with either the full-length wild-type SEMA7A (WT) plasmid or a plasmid with a mutation at the start of the 5′UTR GGCTG—[CT/GT]n—GCC motif (AA). Cells were treated with the inhibitor of the p70S6K (PF-4708671, 10 μM), or with the vehicle only (DMSO). Twenty-four hours after transfection and treatment, cell lysates were prepared and western-blots were performed to quantify SEMA7A, phosphorylated RPS6 (P-RPS6 at S235/S236) and ß-actin. **A**/shows one representative western-blot. **B**/shows the mean ± SD of 3 experiments with ß-actin as control. * Indicates that inhibition of S6K significantly decreases sema7A-WT protein production ($p < 0.04$, *t*-test, $n = 3$). Conversely, the mutated transcript (AA) is highly translated with or without S6K activity. C/SEMA7A transcript levels were quantified by qPCR, 24 h after transfection. Unlike the protein amount, the expression level of the wild-type SEMA7A mRNA is not changed by S6K inhibition, demonstrating controlled protein production at the translation level.

form a double-helix stem and a single-stranded loop [Fig. 6 (Gulia et al., 2020; Kohn et al., 2013; Kowalski and Krude, 2015);]. In between GGCTG and GCC, RNY3 also possesses repeats of [(C/G)T(C/G)] at the intersection of the stem part with the loop [Fig. 6 (Kohn et al., 2013);] .

4. Discussion

In this study, we discovered a motif in the 5′UTR of certain protein-coding mRNAs that are known to have key biological functions in human eosinophils and some other cells. Translation of these mRNAs, including SEMA7A, is known to be controlled by p90S6K. Furthermore, using an easy-to-transfect HeLa cell line, we demonstrated that mutation of the highly conserved beginning of the motif leads to an increased production of protein in the absence of S6K activity without affecting mRNA expression level, suggesting that the start of this sequence is required to reduce mRNA translation rate in the absence of S6K/RPS6 activation. Altogether, these new data from HeLa cells, explain our previous findings in IL3-activated human eosinophils where inhibition of p90S6K activity led to 5-fold reduction of newly synthesized SEMA7A protein, without any change in SEMA7A mRNA level (Esnault et al., 2015).

Using the three 5′UTR sequences of mRNAs regulated at the translational level in activated eosinophils, we identified the consensus sequence motif as GGCTG—$[(C/G)T(C/G)]_n$—GCC. It is important to note that among these three mRNAs, the enhanced mRNA translation of SEMA7A and FCGR2B has a critical implication in the function of eosinophils, particularly in their migration, adhesion, degranulation, release of DNA traps and cytolysis (Esnault et al., 2014, 2017a, 2022). We found that this motif is also present in other mRNAs whose corresponding protein levels are upregulated after eosinophil stimulation. Among these, NFE2 provides cytoprotection against oxidation and cell death (Tan et al., 2018). Also, CD58 via its interaction with CD2 has a critical role in the development of T2 airway inflammation and mucus production (Hashem et al., 2020). In addition, beyond the immune response, we think that this motif may have a broader impact on human health. For instance, we observed the same motif (GGCTG——GCC) in the short 5'UTR of glucose-regulated preproinsulin mRNA, which translation is also controlled by a 5′UTR sequence (Wicksteed et al., 2007).

To demonstrate the importance of this newly identified motif for the regulation of SEMA7A protein synthesis, we found that one mutation (GG- > AA) in the start of the motif (**GG**CTG) resulted in the loss of S6K-dependent mRNA translation. This finding coupled with the predicted secondary structure of the 5′UTR of SEMA7A suggests that a small stem-hairpin loop created by the start of the sequence motif (Fig. 5C) dampens mRNA translation in absence of S6K activation. The insertion of the whole 5′UTR of SEMA7A in the 5′UTR of eGFP construct, containing additional short sequence upstream of the AUG start codon, changes a predicted 5′UTR secondary structure from a small hairpin loop to a long stem with the second loop. Accordingly, it needed a double rather than a single mutation in the sequence motif to lose the requirement for S6K activation. This implies that the nucleotide sequences of the 5′UTR around the

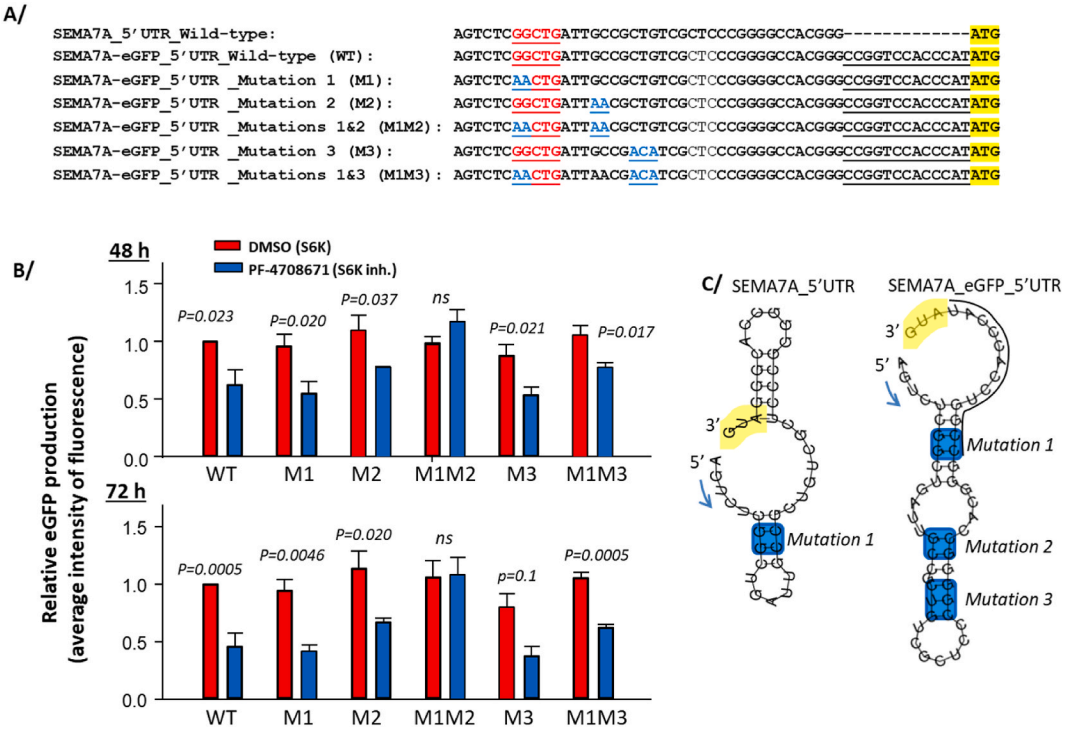

Fig. 5. Mutations in the newly identified motif of SEMA7A 5′UTR upstream of eGFP start codon leads to S6K-independent protein translation. **A**/illustration of the mutations performed in the newly identified motif in the 5′UTR of SEMA7A inserted upstream of eGFP. **B**/After transfection of the constructs in HeLa cells, fluorescence was acquired using fluorescence microscope (EVOS M5000 imaging system, Thermo Fischer, MA, USA). Average intensity of eGFP fluorescence obtained 48 h and 72 h with the mutated plasmids (M1, M2, M1M2, M3 and M1M3) with or without S6K inhibition (PF-4708671) were relative to eGFP protein amount from SEMA7A-eGFP 5′UTR wild-type (WT) that was fixed at 1. The graph shows averages ± SEM of 3 experiments with 5 wells per condition in each experiment. The *t*-test was used to compare S6K versus S6K inhibition for each mutated plasmid, and *p* values are shown. **C**/putative structures of SEMA7A_5′UTR wild-type and SEMA7A-eGFP wild-type were generated using the RNAfold software at http://rna.tbi.univie.ac.at/cgi-bin/RNAWebSuite/RNAfold.cgi. Sites of the 3 mutations are shown in blue squares and the start codon is shown in yellow.

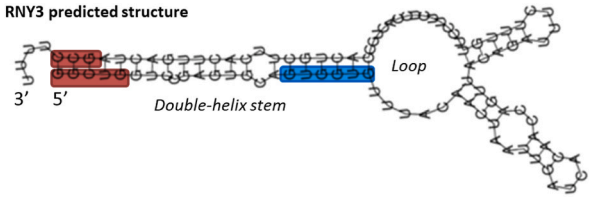

Fig. 6. RNY3 sequence and putative structure. Predicted structure of RNY3 using the RNAfold software at http://rna.tbi.univie.ac.at/cgi-bin/RNAWebSuite/RNAfold.cgi. Similar sequences present in our newly identified motif are shown in red and blue.

newly identified motif are critical to localize the part(s) of the sequence that is(are) necessary for the control of protein synthesis by S6K. Further studies are needed to identify this(these) part(s) in the 5′UTR motif in other transcripts, including FCGR2B and TGFA.

The similarity of the newly identified motif with the non-coding RNY3 full-length sequence is very intriguing. Proteins that regulate structure and functions of RNY3 and bind to the pyrimidine-rich single-stranded loop of RNY3 include, NCL (nucleolin), PTBP1 (huRNP1), HNRNPK, ZBP1, ELAVL4 (HuD), RPL5 (L5), FIP1L1, CPSFs, RNASEL and SYMPK (Gulia et al., 2020; Kohn et al., 2013). Other proteins such as APOBEC3F/G, CARL, IFIT5, ELAVL1 (HuR), MOV10 and YBX1 bind to unknown sites on RNY3 (Gulia et al., 2020; Stake et al., 2015). Among these RBPs, eosinophils express nucleolin, HuR and YB-1 (Capowski et al., 2001; Esnault and Malter, 2003; Shen et al., 2005). Therefore, we may speculate that some of these RBPs regulate the protein production via the newly identified motif.

Downstream the S6 kinases, RPS6 is one of the rare ribosomal proteins to be phosphorylated following cellular stimulation in eukaryotic cells (Evans and Farrar, 1987; Thomas et al., 1982). It has been proposed that phosphorylated RPS6 favors the 40S ribosomal subunit assembly and the formation of polyribosomes (Duncan and McConkey, 1982; Nygard and Nika, 1982), and Roux et al. have showed that p90S6K-phosphorylated RPS6 (Ser235/Ser236) is recruited to the 7-methylguanosine cap structure of mRNAs (Roux

et al., 2007). Interestingly, blockade of RPS6 phosphorylation *in vivo* slightly enhanced rather than reduced the global rate of protein synthesis (Ruvinsky et al., 2005), suggesting that RPS6 phosphorylation may favor the translation of specific mRNAs to the detriment of global protein translation. Specific direct interaction of RPS6 with the newly identified motif or indirect interaction via RBPs will be the subjects for future investigations.

5. Conclusion

We have identified a new conserved sequence motif that regulates protein synthesis in an S6K-dependent manner in the 5′UTR of SEMA7A. This element displays similarities with the small non-coding RNA, RNY3, and likely causes the formation of stem-loops in the 5′UTR of mRNAs via GC-rich sequences. We may speculate that the newly identified motif requires RPS6 activity for maximal mRNA translation.

Author contributions

H.C.S, Y.A.B., J.E.G., N.N.J. and S.E. participated in the conceptualization of the study; H.C.S, Y.A.B., K.S.K., N.N.J. and S.E. designed and/or performed the experiments; H.C.S, Y.A.B., K.S.K., J.E.G., N.N.J. and S.E. analyzed/interpreted the experiments; S.E. prepared the original draft; All authors have reviewed and edited the original draft. All authors have read and agreed to this version of the manuscript.

Grant support

This work was supported by Program Project Grant P01 HL088594; Clinical and Translational Research Center grant UL1 RR025011, U19 AI104317 and R01 AI148707 from the National Institutes of Health; and the Division of Allergy, Pulmonary & Critical Care Medicine of the Department of Medicine at the University of Wisconsin-Madison.

Declaration of competing interest

Nizar N. Jarjour has received consulting fees from Glaxo Smith Kline (GSK), Astra-Zeneca, and Boehringer Ingelheim over the past three years. These relationships with pharmaceutical companies are not relevant to the current study. The remaining authors declare no conflict of interest.

Data availability

Data will be made available on request.

Acknowledgements

The authors would like to thank Shakher Sijapati for his excellent technical assistance.

Appendix A. Supplementary data

Supplementary data to this article can be found online at https://doi.org/10.1016/j.jbior.2023.100975.

References

Capowski, E.E., Esnault, S., Bhattacharya, S., Malter, J.S., 2001. Y box-binding factor promotes eosinophil survival by stabilizing granulocyte-macrophage colony-stimulating factor mRNA. J. Immunol. 167 (10), 5970–5976.

Ding, Y., Tang, Y., Kwok, C.K., Zhang, Y., Bevilacqua, P.C., Assmann, S.M., 2014. In vivo genome-wide profiling of RNA secondary structure reveals novel regulatory features. Nature 505 (7485), 696–700. https://doi.org/10.1038/nature12756. PubMed PMID:24270811.

Duncan, R., McConkey, E.H., 1982. Preferential utilization of phosphorylated 40-S ribosomal subunits during initiation complex formation. Eur. J. Biochem./FEBS 123 (3), 535–538. PubMed PMID: 7075598.

Esnault, S., Fichtinger, P.S., Barretto, K.T., Fogerty, F.J., Bernau, K., Mosher, D.F., Mathur, S.K., Sandbo, N., Jarjour, N.N., 2022. Autophagy protects against eosinophil cytolysis and release of DNA. Cells 11 (11). https://doi.org/10.3390/cells11111821. PubMed PMID: 35681515; PMCID: PMC9180302.

Esnault, S., Hebert, A.S., Jarjour, N.N., Coon, J.J., Mosher, D.F., 2018. Proteomic and phosphoproteomic changes induced by prolonged activation of human eosinophils with IL-3. J. Proteome Res. 17 (6), 2102–2111. https://doi.org/10.1021/acs.jproteome.8b00057. PubMed PMID: 29706072; PMCID: 5984179.

Esnault, S., Johansson, M.W., Kelly, E.A., Koenderman, L., Mosher, D.F., Jarjour, N.N., 2017a. IL-3 up-regulates and activates human eosinophil CD32 and alphaMbeta2 integrin causing degranulation. Clin. Exp. Allergy 47 (4), 488–498. https://doi.org/10.1111/cea.12876. PubMed PMID: 28000949; PMCID: 5378663.

Esnault, S., Kelly, E.A., Johansson, M.W., Liu, L.Y., Han, S.-H., Akhtar, M., Sandbo, N., Mosher, D.F., Denlinger, L.C., Mathur, S.K., Malter, J.S., Jarjour, N.N., 2014. Semaphorin 7A is expressed on airway eosinophils and upregulated by IL-5 family cytokines. Clin. Immunol. 150 (1), 90–100. https://doi.org/10.1016/j.clim.2013.11.009. PubMed PMID: 24333536; PMCID: 3947215.

Esnault, S., Kelly, E.A., Shen, Z.J., Johansson, M.W., Malter, J.S., Jarjour, N.N., 2015. IL-3 maintains activation of the p90S6K/RPS6 pathway and increases translation in human eosinophils. J. Immunol. 195 (6), 2529–2539. https://doi.org/10.4049/jimmunol.1500871. PubMed PMID: 26276876; PMCID: 4561194.

Esnault, S., Malter, J.S., 2003. Hyaluronic acid or TNF-alpha plus fibronectin triggers granulocyte macrophage-colony-stimulating factor mRNA stabilization in eosinophils yet engages differential intracellular pathways and mRNA binding proteins. J. Immunol. 171 (12), 6780–6787.

Esnault, S., Torr, E.E., Bernau, K., Johansson, M.W., Kelly, E.A., Sandbo, N., Jarjour, N.N., 2017b. Endogenous semaphorin-7A impedes human lung fibroblast differentiation. PLoS One 12 (1), e0170207. https://doi.org/10.1371/journal.pone.0170207. PubMed PMID: 28095470; PMCID: 5240965.

Evans, S.W., Farrar, W.L., 1987. Interleukin 2 and diacylglycerol stimulate phosphorylation of 40 S ribosomal S6 protein. Correlation with increased protein synthesis and S6 kinase activation. J. Biol. Chem. 262 (10), 4624–4630. PubMed PMID: 3494010.

Glisovic, T., Bachorik, J.L., Yong, J., Dreyfuss, G., 2008. RNA-binding proteins and post-transcriptional gene regulation. FEBS Lett. 582 (14), 1977–1986. https://doi.org/10.1016/j.febslet.2008.03.004. PubMed PMID: 18342629; PMCID: 2858862.

Gulia, C., Signore, F., Gaffi, M., Gigli, S., Votino, R., Nucciotti, R., Bertacca, L., Zaami, S., Baffa, A., Santini, E., Porrello, A., Piergentili, R., 2020. Y RNA: an overview of their role as potential biomarkers and molecular targets in human cancers. Cancers 12 (5). https://doi.org/10.3390/cancers12051238. PubMed PMID: 32423154; PMCID: PMC7281143.

Hashem, T., Kammala, A.K., Thaxton, K., Griffin, R.M., Mullany, K., Panettieri Jr., R.A., Subramanian, H., Das, R., 2020. CD2 regulates pathogenesis of asthma induced by house dust mice extract. Front. Immunol. 11, 881. https://doi.org/10.3389/fimmu.2020.00881. PubMed PMID: 32477356; PMCID: PMC7235426.

Jefferies, H.B., Reinhard, C., Kozma, S.C., Thomas, G., 1994. Rapamycin selectively represses translation of the "polypyrimidine tract" mRNA family. Proc. Natl. Acad. Sci. U.S.A. 91 (10), 4441–4445. PubMed PMID: 8183928; PMCID: 43801.

Kang, H.R., Lee, C.G., Homer, R.J., Elias, J.A., 2007. Semaphorin 7A plays a critical role in TGF-beta1-induced pulmonary fibrosis. J. Exp. Med. 204 (5), 1083–1093. https://doi.org/10.1084/jem.20061273. PubMed PMID: 17485510; PMCID: 2118575.

Kohn, M., Pazaitis, N., Huttelmaier, S., 2013. Why YRNAs? About versatile RNAs and their functions. Biomolecules 3 (1), 143–156. https://doi.org/10.3390/biom3010143. PubMed PMID: 24970161; PMCID: PMC4030889.

Kowalski, M.P., Krude, T., 2015. Functional roles of non-coding Y RNAs. Int. J. Biochem. Cell Biol. 66, 20–29. https://doi.org/10.1016/j.biocel.2015.07.003. PubMed PMID: 26159929; PMCID: PMC4726728.

Nygard, O., Nika, H., 1982. Identification by RNA-protein cross-linking of ribosomal proteins located at the interface between the small and the large subunits of mammalian ribosomes. EMBO J. 1 (3), 357–362. PubMed PMID: 6201358; PMCID: 553049.

Pelletier, J., Sonenberg, N., 1985. Insertion mutagenesis to increase secondary structure within the 5' noncoding region of a eukaryotic mRNA reduces translational efficiency. Cell 40 (3), 515–526. https://doi.org/10.1016/0092-8674(85)90200-4. PubMed PMID: 2982496.

Reilkoff, R.A., Peng, H., Murray, L.A., Peng, X., Russell, T., Montgomery, R., Feghali-Bostwick, C., Shaw, A., Homer, R.J., Gulati, M., Mathur, A., Elias, J.A., Herzog, E. L., 2013. Semaphorin 7a+ regulatory T cells are associated with progressive idiopathic pulmonary fibrosis and are implicated in transforming growth factor-beta1-induced pulmonary fibrosis. Am. J. Respir. Crit. Care Med. 187 (2), 180–188. https://doi.org/10.1164/rccm.201206-1109OC. PubMed PMID: 23220917; PMCID: 3570653.

Roux, P.P., Shahbazian, D., Vu, H., Holz, M.K., Cohen, M.S., Taunton, J., Sonenberg, N., Blenis, J., 2007. RAS/ERK signaling promotes site-specific ribosomal protein S6 phosphorylation via RSK and stimulates cap-dependent translation. J. Biol. Chem. 282 (19), 14056–14064. https://doi.org/10.1074/jbc.M700906200. PubMed PMID: 17360704; PMCID: 3618456.

Rubio, C.A., Weisburd, B., Holderfield, M., Arias, C., Fang, E., DeRisi, J.L., Fanidi, A., 2014. Transcriptome-wide characterization of the eIF4A signature highlights plasticity in translation regulation. Genome Biol. 15 (10), 476. https://doi.org/10.1186/s13059-014-0476-1. PubMed PMID: 25273840; PMCID: PMC4203936.

Ruvinsky, I., Sharon, N., Lerer, T., Cohen, H., Stolovich-Rain, M., Nir, T., Dor, Y., Zisman, P., Meyuhas, O., 2005. Ribosomal protein S6 phosphorylation is a determinant of cell size and glucose homeostasis. Genes Dev. 19 (18), 2199–2211. https://doi.org/10.1101/gad.351605. PubMed PMID: 16166381; PMCID: 1221890.

Shen, Z.J., Esnault, S., Malter, J.S., 2005. The peptidyl-prolyl isomerase Pin1 regulates the stability of granulocyte-macrophage colony-stimulating factor mRNA in activated eosinophils. Nat. Immunol. 6 (12), 1280–1287.

Stake, M., Singh, D., Singh, G., Marcela Hernandez, J., Kaddis Maldonado, R., Parent, L.J., Boris-Lawrie, K., 2015. HIV-1 and two avian retroviral 5' untranslated regions bind orthologous human and chicken RNA binding proteins. Virology 486, 307–320. https://doi.org/10.1016/j.virol.2015.06.001. PubMed PMID: 26584240; PMCID: PMC4877169.

Suzuki, K., Okuno, T., Yamamoto, M., Pasterkamp, R.J., Takegahara, N., Takamatsu, H., Kitao, T., Takagi, J., Rennert, P.D., Kolodkin, A.L., Kumanogoh, A., Kikutani, H., 2007. Semaphorin 7A initiates T-cell-mediated inflammatory responses through alpha1beta1 integrin. Nature 446 (7136), 680–684.

Taliaferro, J.M., Lambert, N.J., Sudmant, P.H., Dominguez, D., Merkin, J.J., Alexis, M.S., Bazile, C., Burge, C.B., 2016. RNA sequence context effects measured in vitro predict in vivo protein binding and regulation. Mol. Cell 64 (2), 294–306. https://doi.org/10.1016/j.molcel.2016.08.035. PubMed PMID: 27720642; PMCID: PMC5107313.

Tan, L.H., Bahmed, K., Lin, C.R., Marchetti, N., Bolla, S., Criner, G.J., Kelsen, S., Madesh, M., Kosmider, B., 2018. The cytoprotective role of DJ-1 and p45 NFE2 against human primary alveolar type II cell injury and emphysema. Sci. Rep. 8 (1), 3555. https://doi.org/10.1038/s41598-018-21790-3. PubMed PMID: 29476075; PMCID: PMC5824795.

Thomas, G., Martin-Perez, J., Siegmann, M., Otto, A.M., 1982. The effect of serum, EGF, PGF2 alpha and insulin on S6 phosphorylation and the initiation of protein and DNA synthesis. Cell 30 (1), 235–242. PubMed PMID: 6751557.

Thoreen, C.C., Chantranupong, L., Keys, H.R., Wang, T., Gray, N.S., Sabatini, D.M., 2012. A unifying model for mTORC1-mediated regulation of mRNA translation. Nature 485 (7396), 109–113. https://doi.org/10.1038/nature11083. PubMed PMID: 22552098; PMCID: 3347774.

Tuller, T., Zur, H., 2015. Multiple roles of the coding sequence 5' end in gene expression regulation. Nucleic Acids Res. 43 (1), 13–28. https://doi.org/10.1093/nar/gku1313. PubMed PMID: 25505165; PMCID: PMC4288200.

Wan, Y., Qu, K., Zhang, Q.C., Flynn, R.A., Manor, O., Ouyang, Z., Zhang, J., Spitale, R.C., Snyder, M.P., Segal, E., Chang, H.Y., 2014. Landscape and variation of RNA secondary structure across the human transcriptome. Nature 505 (7485), 706–709. https://doi.org/10.1038/nature12946.PubMed. PMID: 24476892; PMCID: PMC3973747.

Wicksteed, B., Uchizono, Y., Alarcon, C., McCuaig, J.F., Shalev, A., Rhodes, C.J., 2007. A cis-element in the 5' untranslated region of the preproinsulin mRNA (ppIGE) is required for glucose regulation of proinsulin translation. Cell Metabol. 5 (3), 221–227. https://doi.org/10.1016/j.cmet.2007.02.007. PubMed PMID: 17339029.